Biochimica et Biophysica Acta 1807 (2011) 491–502

Contents lists available at ScienceDirect

Biochimica et Biophysica Acta

journal homepage: www.elsevier.com/locate/bbabio

Excess no predisposes mitochondrial succinate–cytochrome *c* reductase to produce hydroxyl radical

Jingfeng Chen [b,1], Chwen-Lih Chen [a,1], B. Rita Alevriadou [b], Jay L. Zweier [b], Yeong-Renn Chen [a,b,*]

[a] Department of Integrative Medical Sciences, Northeastern Ohio Universities, Colleges of Medicine and Pharmacy, Rootstown, OH 44272, USA
[b] Davis Heart and Lung Research Institute, The Ohio State University, Columbus, OH 43210, USA

ARTICLE INFO

Article history:
Received 11 September 2010
Received in revised form 7 March 2011
Accepted 8 March 2011
Available online 13 March 2011

Keywords:
Mitochondria
Electron transport chain
SCR
NO
Hydroxyl radical
EPR spin trapping

ABSTRACT

Mitochondria-derived oxygen-free radical(s) are important mediators of oxidative cellular injury. It is widely hypothesized that excess NO enhances $O_2^{\bullet-}$ generated by mitochondria under certain pathological conditions. In the mitochondrial electron transport chain, succinate–cytochrome *c* reductase (SCR) catalyzes the electron transfer reaction from succinate to cytochrome *c*. To gain the insights into the molecular mechanism of how NO overproduction may mediate the oxygen-free radical generation by SCR, we employed isolated SCR, cardiac myoblast H9c2, and endothelial cells to study the interaction of NO with SCR in vitro and ex vivo. Under the conditions of enzyme turnover in the presence of NO donor (DEANO), SCR gained pro-oxidant function for generating hydroxyl radical as detected by EPR spin trapping using DEPMPO. The EPR signal associated with DEPMPO/$^{\bullet}$OH adduct was nearly completely abolished in the presence of catalase or an iron chelator and partially inhibited by SOD, suggesting the involvement of the iron–H_2O_2-dependent Fenton reaction or $O_2^{\bullet-}$-dependent Haber–Weiss mechanism. Direct EPR measurement of SCR at 77 K indicated the formation of a nonheme iron–NO complex, implying that electron leakage to molecular oxygen was enhanced at the FAD cofactor, and that excess NO predisposed SCR to produce $^{\bullet}$OH. In H9c2 cells, SCR-dependent oxygen-free radical generation was stimulated by NO released from DEANO or produced by the cells following exposure to hypoxia/reoxygenation. With shear exposure that led to overproduction of NO by the endothelium, SCR-mediated oxygen-free radical production was also detected in cultured vascular endothelial cells.

1. Introduction

Mitochondria are the major cellular source of oxygen-free radicals [1,2]. The generation of reactive oxygen species (ROS) and free radical (s) in mitochondria is relevant under the physiological conditions of low oxygen tension such as state 4 respiration and is particularly high under certain pathological conditions such as inflammation and ischemia-reperfusion injury [3–5]. The controlled production of NO, another reactive species, has an important role in the human vascular system [6,7]. NO produced from endothelial cells has the capacity to modulate mitochondrial functions in regulation of respiration and metabolism. It is widely accepted that excessive production of NO can cause cell death (such as myocardial infarction) in human pathology [6,8]. For example, myocardial ischemia–reperfusion provides a stimulus to alter NO metabolism [6,9–11]. Increased production of both $O_2^{\bullet-}$ and NO and subsequent peroxynitrite ($OONO^-$) formation have been marked in the post-ischemic myocardium [12,13].

It has been well documented that NO can reversibly inhibit mitochondrial cytochrome *c* oxidase (C*c*O or complex IV) in competition with oxygen and serve as a physiological regulator of mitochondrial respiration [7,14]. The inhibition of C*c*O by NO, although reversible, can block electron flow of the respiratory chain from either NADH or succinate to molecular oxygen to cause electron accumulation in the ETC and thus increase $O_2^{\bullet-}$ production. Furthermore, succinate–cytochrome *c* reductase (SCR, a supercomplex hosting complex II (succinate ubiquinone reductase, SQR) and complex III (ubiquinol cytochrome *c* reductase, QCR) has been implicated as the other target of NO in cellular respiration [15]. Specifically, it has been reported that excess NO induced by cytokines in smooth muscle cells under inflammatory conditions can regulate mitochondrial respiration through inhibition of complex II.

Physiologically, the SCR supercomplex mediates electron transfer from succinate to cytochrome *c* (cyt *c*) during mitochondrial respiration. The redox centers of SQR contain flavin adenine nucleotide (FAD), three

Abbreviations: SQR, succinate ubiquinone reductase or mitochondrial complex II; SCR, succinate cytochrome *c* reductase or supercomplex containing complex II and complex III; QCR, ubiquinol cytochrome *c* reductase or complex III; ISP, iron sulfur protein; $O_2^{\bullet-}$, superoxide anion; ROS, reactive oxygen species; ETC, electron transport chain; FAD, flavin adenine dinucleotide; DEPMPO, 5-diethoxylphosphoryl-5-methyl-1-pyrroline *N*-oxide; SOD, superoxide dismutase; SDS-PAGE, SDS polyacrylamide gel electrophoresis; EPR, electron paramagnetic resonance; PBS, phosphate buffered saline; DEANO, diethylamine nonoate; SGA, superoxide generation activity; ETA, electron transfer activity; H/RO, hypoxia/reoxygenation; ECs, endothelial cells

* Corresponding author at: Department of Integrative Medical Sciences, Northeastern Ohio Universities, Colleges of Medicine and Pharmacy, Rootstown, OH 44272, USA. Tel.: +1 330 325 6537; fax: +1 330 325 5912.
E-mail address: ychen1@neoucom.edu (Y.-R. Chen).

[1] Both authors contributed equally to this work.

0005-2728/$ – see front matter © 2011 Elsevier B.V. All rights reserved.
doi:10.1016/j.bbabio.2011.03.001

iron-sulfur clusters (S-1, S-2, and S-3), cytochrome b_{560}, and ubiquinone (Q). The redox centers of QCR consist of ubiquinol (QH_2), cytochromes b_L (low potential *b* or b_{566}), b_H (high potential *b* or b_{562}), and c_1, and the Rieske iron-sulfur cluster (RISP). Succinate serves as an electron donor for SQR to reduce FAD, after which an electron is transferred from the reduced FAD to the iron sulfur clusters and cytochrome b_{560}, and Q is reduced to QH_2. The electron transfer from QH_2 to ferricytochrome *c* (cyt *c*) is catalyzed by QCR and follows the Q cycle mechanism.

It has been reported that mediation of $O_2^{\bullet-}$ production by SCR is kept minimized under the conditions of enzyme turnover in the presence of succinate and cyt *c* [16]. Hypothetically, excess NO should out-compete molecular oxygen in binding to CcO (complex IV) and subsequently increase electron leakage from the ETC (see Supplementary Chart). It is expected that excess NO also binds to the SCR and subsequently stimulates the $O_2^{\bullet-}$ production from the SCR in mitochondria as illustrated in the Supplementary Chart. Exposure of SCR to excess NO in vitro resulted in irreversible inhibition of SQR activity in SCR. This inactivation was reported to be due primarily to damage to iron–sulfur clusters from SQR [17]. In the ex vivo cellular studies, excess NO induced by cytokine under inflammatory conditions mediated the formation of iron-nitrosyl intermediate [18,19]. However, the molecular mechanisms are not clear, nor are the toxicological consequences of excess NO-mediated oxidant stress on the SCR. The present study was undertaken to address the fundamental questions regarding the molecular mechanism resulting from the interaction of excess NO with SCR. In vitro studies using the isolated SCR supercomplex have the advantage to provide precise measurements and unequivocal results, which can complement the ex vivo studies using living cells. Based on the studies using purified enzyme supercomplex, we have found that excess NO increased the pro-oxidant activity of SCR and predisposed SCR to be a source of hydroxyl radical due to oxidative damage of the iron sulfur cluster. Based on ex vivo cellular studies using the embryonic cardiomyoblast H9c2 cell line and endothelial cells, we have demonstrated that excess NO emitted by NO donor or produced under the physiological conditions of H/RO (hypoxia-reoxygenation) and shear exposure contributed to SCR-dependent oxygen-free radical production. These findings of in vivo and ex vivo studies were mutually supported and thus offered a strong conclusion in the connection of NO with mitochondrial SCR in the cellular pathophysiological conditions.

2. Materials and methods

2.1. Reagents

Ammonium acetate, ammonium sulfate, diethylenetriaminepentaacetic acid (DTPA), ubiquinone-2 (Q_2), sodium cholate, deoxycholic acid, deferoxamine, Triton X-100, Zn/Cu superoxide dismutase (SOD), bovine apotransferrin, oxaloacetic acid, potassium salt of 2-(4-carboxyphenyl)-4,4,5,5-tetramethylimidazoline-1oxyl-3-oxide (c-PTIO), ebeslen (2-phenyl-1,2-benzisoselenazol-3(2H)-one), and sodium succinate were purchased from Sigma Chemical Company (St. Louis, MO) and used as received. Catalase (bovine liver) was purchased from Roche Diagnostics (Indianapolis, IN). Peroxynitrite and the NO donor diethylamine nonoate (DEANO) were purchased from Cayman Chemical (Ann Arber, MI). The 5-diethoxylphosphoryl-5-methyl-1-pyrroline *N*-oxide (DEPMPO) spin trap and Mn(III) Tetrakis (1-methyl-4-pyridyl) porphyrin pentachloride (MnTMPyP) were purchased from ALEXIS Biochemicals (San Diego, CA).

2.2. Preparations of mitochondrial succinate cytochrome c reductase (SCR) and succinate ubiquinone reductase (SQR) and ubiquinol cytochrome c reductase (QCR)

Bovine heart mitochondrial SCR, SQR, and QCR were prepared and assayed according to the published method developed by Yu et al. [20]. The purified SCR contained 4–4.2 nmol heme *b* per mg protein and exhibited an activity of approximately 8.5 μmol cyt *c* reduced/min/mg protein. Purified SCR was stored in 50 mM Na/K phosphate buffer, pH 7.4, containing 0.25 M sucrose and 1 mM EDTA. The purified SQR has specific activity ~15.2 μmol of succinate oxidized (or dichlorophenol indophenol, DCPIP, reduced)/min/mg protein. The purified QCR has specific activity ~8.0 μmol of cyt *c* reduced/min/nmol cyt *b*.

2.3. Analytical methods

Optical spectra were measured on a Shimadzu 2401 UV/VIS recording spectrophotometer. The enzyme concentration (based on the heme *b*) of SCR was calculated from the differential spectrum between dithionite reduction and ferricyanide oxidation, using an extinction coefficient of 28.5 mM^{-1} cm^{-1} for the absorbance difference of $A_{562nm} - A_{576nm}$. The enzyme activity of SCR was assayed by measuring cyt *c* reduction. An appropriate amount of SCR was added to an assay mixture (1 ml) containing 50 mM phosphate buffer, pH 7.4, 0.3 mM EDTA, 19.8 mM succinate, and 50 μM ferricytochrome *c*. The SCR activity was determined by measuring the increase in absorbance at 550 nm. The enzymatic activity of SQR was assayed by measuring Q_2-stimulated DCPIP reduction by succinate as described in the literature [20]. QCR activity was assayed by Q_2H_2-mediated ferricytochrome *c* reduction at room temperature [20].

The heme *b* concentration of SCR was calculated from the differential spectrum between dithionite reduction and ferricyanide oxidation. The NO released from DEANO in PBS was measured at 25 °C (in PBS) or 37 °C (in the cell culture medium) in a water-jacketed electrochemical vial using a Clark-type NO electrode (ISO-NOP) from World Precision Instruments (WPI, Sarasota, FL). The solution (2 ml) measured in the vial was constantly stirred with a magnetic bar controlled by a stirrer under the vial. The current collected by the NO electrode, which was proportional to the NO concentration in the solution, was recorded with an Apollo 4000 Free Radical Analyzer from WPI. The NO electrode was calibrated with known concentrations of NO, using NO-equilibrated solutions as described in the literature [21].

2.4. Electron paramagnetic resonance measurements

EPR measurements were performed on a Bruker EMX spectrometer operating at 9.86 GHz with 100 kHz modulation frequency at room temperature. The reaction mixture was transferred to a 50 μl capillary, which was then positioned in an HS cavity (Bruker Instrument, Billerica, MA). The sample was scanned using the following parameters: center field, 3510 G; sweep width, 140 G; power, 20 mW; receiver gain, 2×10^5; modulation amplitude, 1 G; time of conversion, 163.84 ms; time constant, 163.84 ms; number of scans, 4 scans. The spectral simulations were performed using the WinSim program developed at NIEHS by Duling [22]. The hyperfine coupling constants used to simulate the spin adduct of DEPMPO/$^{\bullet}$OOH were as follows: isomer 1: $a^N = 13.14$ G, $a^H_{\beta} = 11.04$ G, $a^H_{\gamma} = 0.96$ G, $a^P = 49.96$ G; isomer 2: $a^N = 13.18$ G, $a^H_{\beta} = 12.59$ G, $a^H_{\gamma} = 3.46$ G, $a^P = 48.2$ G; DEPMPO/$^{\bullet}$OH, $a^N = 14.03$ G, $a^H_{\beta} = 13.34$ G, $a^P = 47.19$ G [23,24].

2.5. Measurement of NO-induced oxygen-free radical(s) mediated from SCR in H9c2 living cells

Rat embryonic cardiomyoblasts (H9c2 cell line from ATCC, Manassas, VA) were grown and maintained in Dulbecco's modified Eagle's medium supplemented with 5% fetal bovine serum and 1% penicillin/streptomycin antibiotics in 35-mm polystyrene tissue culture dishes at 37 °C in the presence of 4.5% CO_2. Confluent cells with >90% viability were used to conduct fluorescence imaging of $O_2^{\bullet-}$ production in living cells.

H9c2 cells were then cultured on sterile coverslips in 35-mm sterile dishes at a density of 10^4 cells/dish and subjected to DEANO (10 μM) treatment for 20 min at 37 °C. To measure the contribution of SCR in the $O_2^{\bullet-}$ production induced by DEANO, H9c2s were treated with OAA

(100 μM), a competitive inhibitor of succinate dehydrogenase from the TCA cycle (Supplementary Chart). To verify the effect of NO generated from DEANO, H9c2s were incubated with 2-(4-carboxyphenyl)-4,5-dihydro-4,4,5,5-tetramethyl-1H-imidazolyl-1oxy-3oxide (Carboxy-PTIO), an NO scavenger. Cells were then incubated with the $O_2^{\bullet-}$ indicator 5 μM MitoSOX™ (Molecular Probes, Inc., Eugene OR; a red mitochondrial oxygen-free radical indicator for live-cell images) to detect $O_2^{\bullet-}$ in living cells. MitoSOX™ red fluorescences (Ex/Em 510/580 nm) when oxidized by $O_2^{\bullet-}$. Nuclei were stained with blue fluorescence DAPI (1 μM) for 10 min in the incubator. After the incubation, cells were washed twice with PBS and mounted using a mounting medium of fluoromount-G, and images were captured and analyzed at a magnification of 20× for MitoSOX™ and DAPI by confocal fluorescence microscopy (LSM 510; Zeiss Inc., Peabody, MA) and overlaid using LSM software.

Hypoxic treatment was accomplished by placing cells in a Modular Incubator Chamber (Billups-Rothenberg, Inc., Del Mar, CA) and incubating for 1 h while flushing nitrogen gas on the surface of glucose-free medium, after which reoxygenation was carried out by incubating in medium with glucose for 3 min.

2.6. EC culture and exposure to shear stress

Primary bovine aortic endothelial cells (BAECs) were purchased from Cambrex (East Rutherford, NJ) and cultured in Dulbecco's modified Eagle's medium (DMEM) with L-glutamine and $NaHCO_3$ supplemented with 10% fetal bovine serum (FBS) and antibiotics. ECs (passages 3–6) were seeded onto glass slides (75 × 38 mm; Fisher Scientific, Pittsburgh, PA) that were sterilized, air-dried and coated with a 0.5% gelatin subbing solution that contained 0.05% potassium chromium sulfate (Sigma, St. Louis, MO). EC monolayers were used within 24 h upon confluence. ECs were incubated overnight in the same medium as the culture medium, except that DMEM was phenol red-free and FBS was 2%, and exposed to shear stress in the same with the overnight incubation medium. For shear exposure, three glass slides with EC monolayers were assembled side-by-side into a parallel-plate flow chamber, and the chamber was connected at both ends to a reservoir forming a flow loop. In this setup, ECs were exposed to a constant gravity-driven laminar shear stress of 10 dyn/cm^2 (low arterial range) for 30 min, as described before [25]. Flow rate through the chamber was monitored by an ultrasonic flow sensor (Transonic Systems, Ithaca, NY). Recirculating culture medium was constantly exposed to a counter-current flow of a sterile-filtered gas mixture (95% air–5% CO_2) that was warmed and humidified by bubbling through water; this permitted the use of protein-rich medium (with ≤10% FBS) without foaming. Medium O_2 concentration and temperature were monitored real-time by inline optical O_2 and temperature sensors (WPI). The temperature of the entire system was kept at 37 °C. Corresponding static controls were preincubated and maintained in the incubator for the same time periods and in the same medium as the perfusion medium. Some EC monolayers were preincubated with either an eNOS inhibitor (1 mM of L-NAME for 1 h) or OAA (100 μM for 1 h).

3. Results

3.1. Measurement of NO production from DEANO in PBS by electrochemical detection

Diethylamine NONOate (DEANO) has been widely used as an NO donor. DEANO releases a short-term burst of NO, which should be relevant in acute pathophysiological conditions such as shear exposure and hypoxia/reoxygenation. In order to use DEANO as an NO generator in the reaction system, we must measure the amount of NO released from DEANO in PBS; we chose electrochemical detection using an NO electrode as a powerful and sensitive approach to quantify NO released from DEANO in PBS at 25 °C and to monitor the rate of its decay. When DEANO (10, 25, and 50 μM) was added to the PBS solution, the maximal concentration of NO generated from DEANO was calculated to be 1.2 (measured at time point between 4.5 and 5.5 min), 3.6 (measured at the time point between 4.1 and 4.7 min), and 5.8 μM (measured at the time point between 3.2 and 3.6 min) (Supplementary Fig. 1).

3.2. DEPMPO spin-trapping hydroxyl radical generated from SCR under the conditions of enzyme turnover in the presence of DEANO

To measure the molecular mechanism of interaction of NO with mitochondrial SCR unambiguously, we isolated the supercomplex SCR from bovine hearts and used it to evaluate the effect of NO on SCR in vitro. It has been reported that $O_2^{\bullet-}$ generation mediated by SCR was minimal under the conditions of enzyme turnover in the presence of succinate and cyt *c* ([16]; Fig. 1D). The NO donor, DEANO was incubated with a solution containing SCR (2 μM, based on heme *b*) at room temperature. When the DEANO-inhibited SCR was activated with succinate in the presence of cyt *c* and DEPMPO, an eight-line EPR spectrum with an intensity ratio of 1:2:2:1:1:2:2:1 was detected (Fig. 1A–C, solid line). Based on the literature and computer simulation (Fig. 1A–C, dashed line), this spectrum was assigned to the DEPMPO-hydroxyl radical adduct (DEPMPO/$^{\bullet}$OH, $a_N = 14.0$ G; $a_H = 13.2$ G; $a_P = 47.3$ G). It is important to note that production of SCR-mediated DEPMPO/$^{\bullet}$OH adduct can be detected at the dosage of DEANO concentration as low as 10 μM, generating maximal steady-state NO concentration of 1.4 ± 0.2 μM that is close to pathophysiological level (Fig. 1A).

The detected DEPMPO/$^{\bullet}$OH was entirely dependent on the presence of both DEANO and SCR (Fig. 1D–E). In the presence of catalase or an iron chelator (deferoxamine, DFO), the EPR signal associated with DEPMPO/$^{\bullet}$OH was attenuated by more than 95% (Fig. 1F), suggesting the involvement of the iron–H_2O_2-dependent Fenton reaction in the hydroxyl radical production. Transferrin is the blood plasma protein which binds avidly free iron, but is redox inactive at the state of iron-free or iron-complexed. Addition of apotransferrin to the system inhibited more than 80% of DEPMPO/$^{\bullet}$OH adduct formation (Fig. 1F), thus eliminating the possibility of deferoxamine's antioxidant property independent of its iron chelation effects [26]. However, the detected DEPMPO/$^{\bullet}$OH was only partially inhibited by SOD (~65% inhibition; Fig. 1F), indicating the involvement of $O_2^{\bullet-}$-dependent Haber–Weiss mechanism in the SCR-mediated hydroxyl radical production. The detected DEPMPO/$^{\bullet}$OH was enhanced by ~23.4% when cyt *c* was omitted from the system (data not shown), suggesting scavenging of $O_2^{\bullet-}$ by cyt *c* partially diminished the pathway of $O_2^{\bullet-}$-dependent hydroxyl radical production. It should be noted that cyt *c* in its oxidized state can bind NO and in its reduced state can react with NO ($k = 200\ M^{-1}\ s^{-1}$) to form a species with $OONO^-$-like activity, which may also contribute to the hydroxyl radical formation [27].

To provide a solid evidence of trapping $^{\bullet}$OH generated from DEANO-treated SCR, we have carried out the same experiment using DMPO (100 mM) as the spin trap, a four-line spectrum with an intensity ratio of 1:2:2:1 was detected (Fig. 1G). This spectrum was assigned to the DMPO-hydroxyl radical adduct with a hyperfine coupling constants $a_N = 14.85$ G; $a_H = 14.85$ G. We then added the well known hydroxyl radical scavenger Me_2SO (DMSO, 10% v/v) to the system. The EPR spectrum recorded (Fig. 1H, solid line) was simulated as a combination of two DMPO radical adducts (Fig. 1H, dashed line). The first adduct was assigned to DMPO/methyl radical (DMPO/$^{\bullet}CH_3$) based on the hyperfine coupling constants $a_N = 16.1$ G; $a_H = 23.0$ G (Fig. 1I). The second adduct was assigned to DMPO/$^{\bullet}$OH (Fig. 1J). The intensity of DMPO/$^{\bullet}$OH adduct was inhibited due to Me_2SO scavenging of hydroxyl radical, yielding a 6-line spectrum of DMPO/$^{\bullet}CH_3$.

3.3. An intact supercomplex is required for SCR-mediated hydroxyl radical generation induced by DEANO

The supercomplex SCR hosts both SQR (complex II) and QCR (complex III). The enzymatic activity of SCR in catalyzing electron

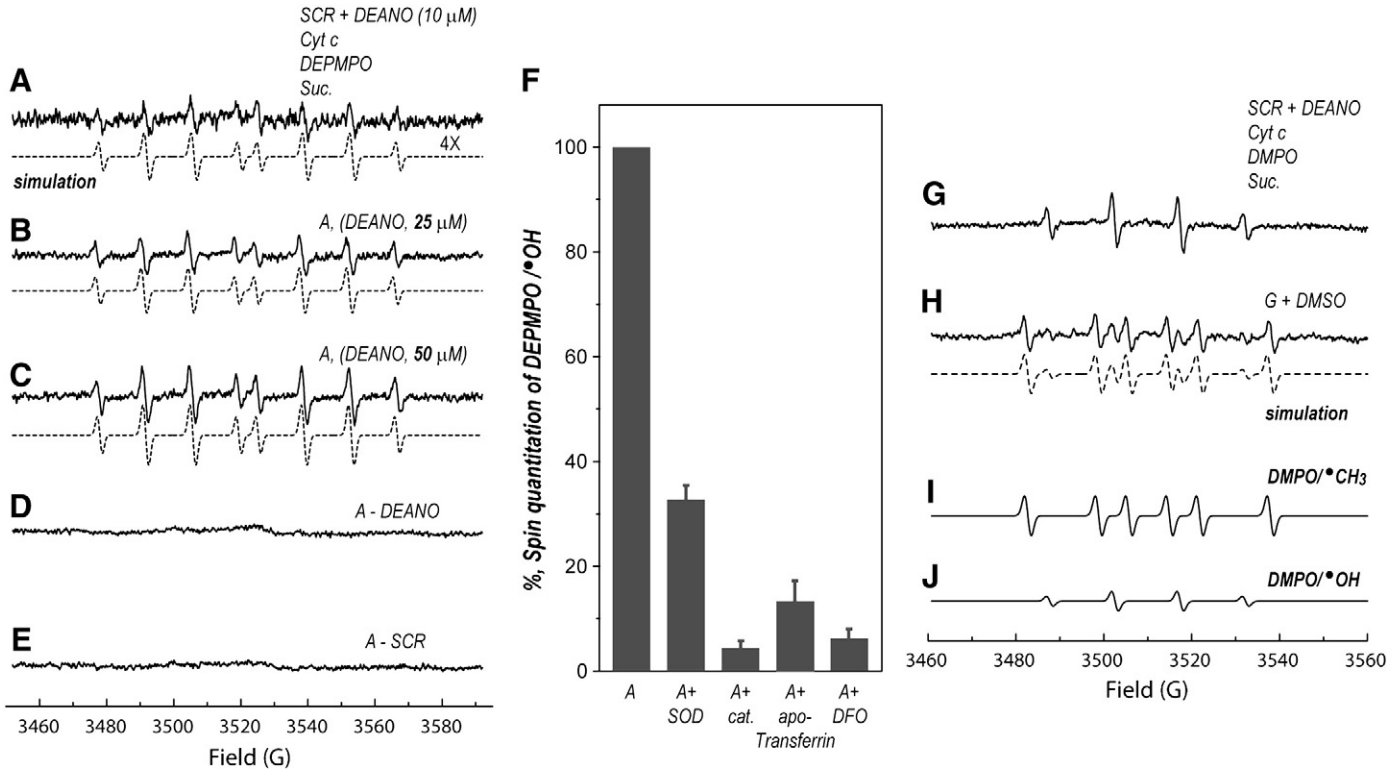

Fig. 1. EPR spin trapping of •OH generated from SCR under the conditions of enzyme turnover in the presence of DEPMPO (A–F) or DMPO (G–H) and the NO generator DEANO. (A-C, E, and G-H) The computer simulation (dashed line) superimposed on the experimental spectrum (solid line) obtained using SCR (2 μM), succinate (18 μM), and cyt *c* (6 μM), various concentration of DEANO (10, 25, and 50 μM), and DEPMPO (20 mM) in PBS. Note that SCR was pre-incubated with DEANO at room temperature for 1 min prior to addition of substrates and spin trap. The experimental spectrum was recorded after signal averaging five scans at room temperature. (D) The same as A–C, except that the DEANO was omitted from the system. (E) The same as A–C, except that the enzyme was omitted from the system. (F) Effect of catalase (5 U/μl), superoxide dismutase (SOD, 2 U/μl), apotransferrin (1 mg/ml), and deferoxamine (DFO, 1 mM) on DEPMPO/•OH production in the reaction system of C. (G) Same as C, except that DEPMPO was replaced with DMPO (100 mM). (H) Same as G, except that DMSO (10% v/v) was included in the system prior to EPR measurement. The computer simulated spectrum (dashed line) is superimposed on the experimental spectrum (solid line). (I and J) Individual simulations of each species in the composite spectrum.

transfer from succinate to cyt *c* can be reconstituted by SQR and QCR [20]. To know whether an intact supercomplex of SCR is absolutely required for the detected hydroxyl radical generation by SCR in the presence of DEANO, SQR and QCR were isolated from myocardial tissue according to a published procedure [20]. As indicated in Fig. 2A, SQR-mediated $O_2^{\bullet-}$ was detected under conditions of enzyme turnover in the presence of succinate and Q_2. In the presence of the NO donor DEANO, production of $O_2^{\bullet-}$ by SQR was diminished by 39.6% (Fig. 2B), presumably due to trapping of $O_2^{\bullet-}$ by NO. A similar situation was also observed in the QCR (complex III) when $O_2^{\bullet-}$ production was generated under the turnover conditions in the presence of ubiquinol-2 (Q_2H_2) and cyt *c* (Fig. 2C–D). Note that incubation of Q_2H_2 and spin trap did not yield a detectable DEPMPO/•OOH adduct (Fig. 2E), thus eliminating the possibility of $O_2^{\bullet-}$ generated from Q_2H_2 autooxidation. When isolated SQR was reconstituted with QCR in vitro, the catalytic activity of SCR was restored [20]. Under the conditions of enzyme turnover in the presence of succinate and cyt *c*, $O_2^{\bullet-}$ production mediated by reconstituted SCR was not detected (Fig. 2F), a result consistent with the observation in intact SCR (Fig. 1D) [16]. In the presence of DEANO and DEPMPO, the electron transfer activity of reconstituted SCR was inhibited and an eight-line spectrum of DEPMPO/•OH was detected (Fig. 2G), confirming that the formation of *intact* supercomplex was required for SCR-mediated hydroxyl radical production (as indicated in the Fig. 1A–C).

3.4. Effect of TTFA and succinate dosage on the SCR-mediated hydroxyl radical formation in the presence of DEANO and cyt c

The enzymatic activity of SQR in SCR is sensitive to thenoyl trifluoroacetone (TTFA), which inhibits electron transfer from SQR to QCR via binding to the S3 center and the cytochrome b_{560} in SQR [28]. The addition of TTFA (1 mM) in the reaction system significantly inhibited the formation of hydroxyl radical adduct of DEPMPO (~83.1% inhibition based on computer simulation and spin quantitation by double integration of simulated spectra, dashed lines of Fig. 3A and B), but resulting in the detection of superoxide radical adduct of DEPMPO (solid line in the Fig. 3B), implying that most electron leakage is occurred at the FAD cofactor of the SQR.

Imlay and coworker have reported that high concentrations of succinate suppress the $O_2^{\bullet-}$ formation by protecting the FAD reaction with O_2 [29]. Higher levels of succinate (2–20 mM) were used to examine the effect on the SCR-mediated DEPMPO/•OH generation. As indicated in the Fig. 3C—E, higher concentrations of succiante suppress most hydroxyl radical formation. Together with the result of TTFA inhibition (Fig. 3B), $O_2^{\bullet-}$-dependent hydroxyl radical production was controlled by FAD cofactor, and low level of succinate (μM range) was not sufficient to saturate the binding site, which would contribute to oxygen-free radical formation mediated by SCR.

3.5. Effect of DEANO on the electron transfer activities of SCR

As shown in the Supplementary Fig. 2A, incubation of DEANO (50 μM) with SCR (2 μM, based on heme *b*) at room temperature for 30 min resulted in the impairment of electron transfer activity from succinate to cyt *c* (SCR, 1.53 ± 0.13 μmol cyt *c* reduced/min/nmol *b*) by 29.7% (SCR+DEANO, 1.07 ± 0.08 μmol cyt *c* reduced/min/nmol *b*, $n = 3$) and impairment of electron transfer activity from succinate to ubiquinone (SQR, 0.57 ± 0.04 μmol DCPIP reduced/min/nmol *b*) by 34.7% (SCR+DEANO, 0.37 ± 0.02 μmol DCPIP reduced/min/nmol *b*, $n = 3$). However, DEANO treatment of SCR did not affect the electron transfer activity from ubiquinol to cyt *c* (QCR, 5.21 ± 0.19 μmol cyt *c*

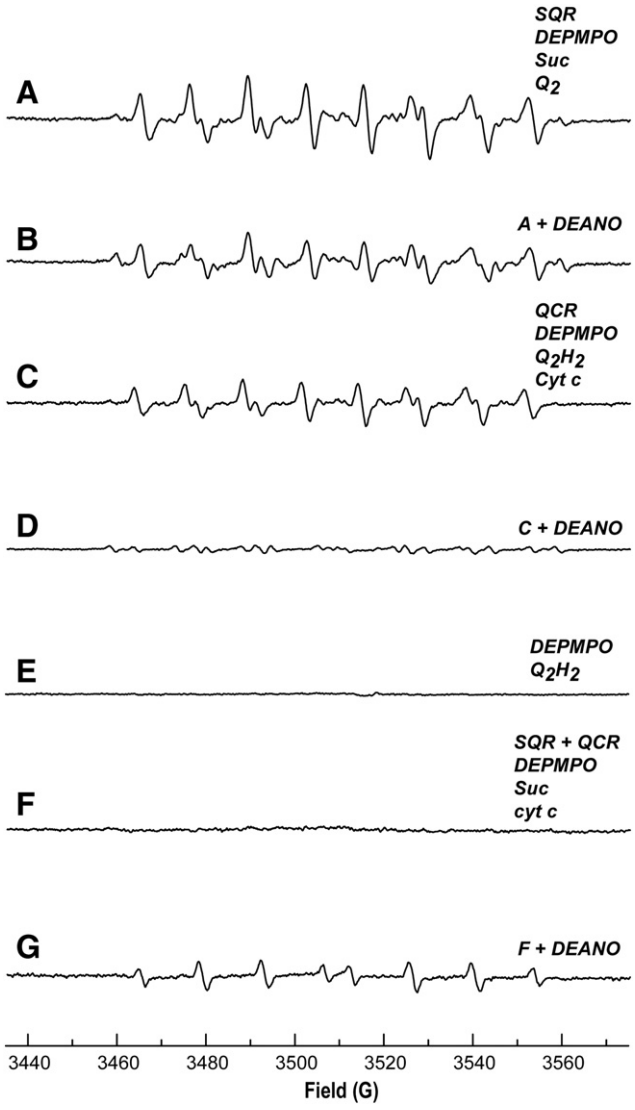

Fig. 2. Effect of DEANO on the oxygen-free radical generation by isolated SQR, isolated QCR, and reconstituted SCR as measured by EPR spin-trapping with DEPMPO. (A) Isolated SQR (1 μM, based on heme *b*) was incubated with Q_2 (0.72 mM) in the presence of DEPMPO (20 mM). The reaction was initiated with the addition of succinate (18 μM) prior to EPR measurement. (B) The same as A, except that DEANO (50 μM) was included in the reaction system. (C) QCR (2 μM, based on heme *b*) was incubated with cyt *c* (10 μM) in the presence of DEPMPO (20 mM), and the reaction was initiated with Q_2H_2 (0.72 mM) prior to EPR measurement. (D) The same as C, except that DEANO (50 μM) was included in the reaction system. (E) The same as C, except that QCR and cyt *c* were eliminated from the system. (F) SQR (1 μM) was reconstituted with the QCR (2 μM, based on heme *b*) at 0 °C for 1 h. Reconstituted SCR was then incubated with cytochrome *c* (10 μM) in the presence of DEPMPO (20 mM), and the reaction was initiated with succinate (18 μM) prior to EPR measurement. (G) The same as F, except that DEANO (50 μM) was included in the reaction system. Note that DEANO was pre-incubated with enzyme at room temperature for 1 min prior to addition of substrates and spin trap in B, D, and G.

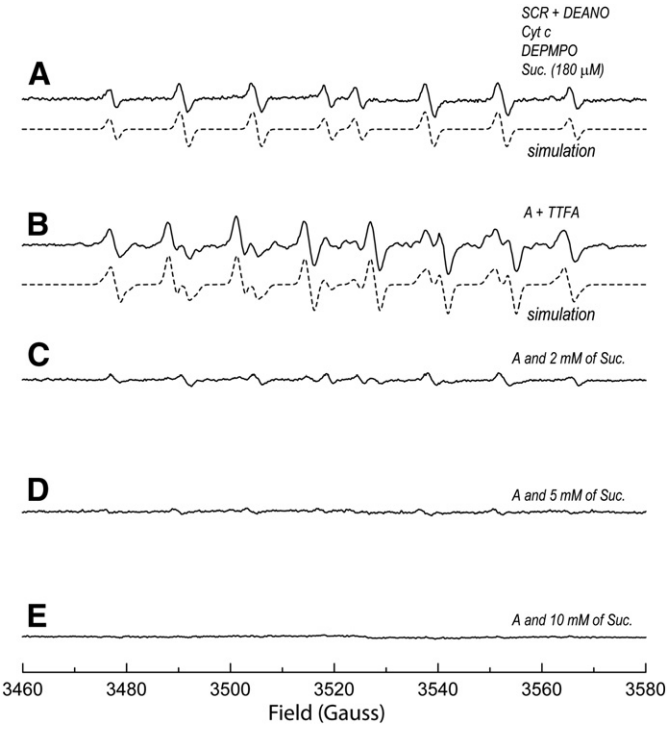

Fig. 3. Effect of TTFA and the dosage of succinate on SCR-mediated ˙OH generation under the conditions of enzyme turnover in the presence DEANO. (A) Computer simulation (dashed line) superimposed on the experimental spectrum (solid line) as described in experimental conditions of Fig. 1A (50 μM of DEANO used). The spin quantitation was obtained by double integration of simulated spectrum. (B) The same as A, except that SCR was pre-incubated with TTFA (1 mM). Based on the simulated spectrum (dashed line), the molar ratio for the two species is 0.988 for DEPMPO/˙OOH, and 0.012 for DEPMPO/˙OH. The spin quantitation was obtained by double integration of simulated spectrum. (C–E) The same as A, except that the dosage of succinate was increased to 2 mM, 5 mM, and 10 mM respectively.

reduced/min/nmol *b*) to a significant level. These results indicate that DEANO-mediated SCR inhibition is primarily caused by the interaction of NO with the SQR moiety of SCR. Note that hemes *b* and c_1 are mainly presented as the oxidized state in the absence of succinate. The addition of DEANO did not affect on the heme spectrum (Supplementary Fig. 2B), indicating no interaction between NO and the heme *b* and heme c_1 of SCR.

3.6. Effect of DEANO in the succinate-induced heme b reduction of SCR

To understand how NO released from the DEANO affecting the heme *b* reduction of SCR, we employed UV/vis spectroscopy. As indicated by UV/Vis spectra (Supplementary Fig. 2C), complete reduction of heme *b* and heme c_1 was achieved by sodium dithionite (Supplementary Fig. 2C, dashed line). Addition of excess succinate (1 mM) to native SCR resulted in the partial reduction of heme *b* (λmax=562 nm) and c_1 (λmax=552 nm) in SCR (Supplementary Fig. 2C, solid line). When SCR was pretreated with the NO donor DEANO (10–100 μM), the addition of excess succinate partially inhibited the heme *b* reduction found using native SCR (decreased by 49.7 ± 0.6%, $n=3$, compared to heme *b* reduction), indicating heme *b* was being differentially reduced in the presence of DEANO. Complete reduction of DEANO-treated SCR was achieved by sodium dithionite. These results, in part, supported that succinate-induced electron transfer from FAD to heme *b* in SCR was interrupted by NO released from the DEANO.

3.7. Detection of NO–iron complex of SQR from the reaction of DEANO with SCR in the presence of succinate

The X-band EPR spectrum of succinate-reduced SCR obtained at 77 K is characteristic of iron sulfur clusters from complex II in the reduced state. It represents distinct ferredoxin-type iron–sulfur centers with magnetic field parameters $g_z=2.03$, $g_y=1.93$, and $g_x=1.91$ (Fig. 4A) [17,30]. In the presence of excess DEANO (12.5-fold excess), the characteristic signal of the EPR spectrum was converted to that of an NO–iron complex with the magnetic field parameter $g=2.05$ (Fig. 4B), presumably due to the formation of a dinitrosyl-iron complex at the reduced S-1 center [2Fe–2S] of complex II [17,31]. The result suggested that formation of dinitrosyl-iron complex in the SCR subsequently blocked electron flow from succinate to cyt *c*, and enhanced electron leakage from FAD cofactor under the conditions of enzyme turnover. The involvement of the iron–H_2O_2-dependent Fenton reaction in the detected hydroxyl radical production also implies that excess amount

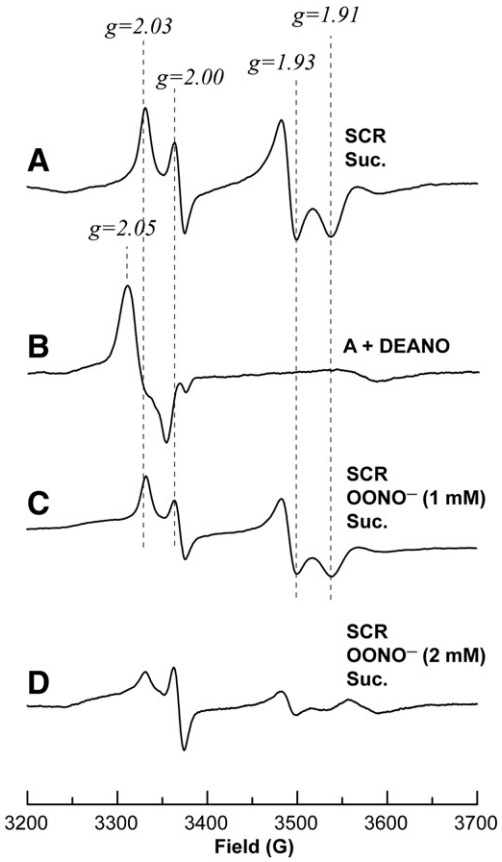

Fig. 4. Effect of NO on the EPR spectrum of the iron sulfur cluster (S1 center) of succinate-reduced SCR at 77 K. (A) The reaction mixture contained SCR (80 μM, based on heme *b*) in 50 mM Tris-Cl, pH 8.0 containing 0.66 M sucrose and 20% glycerol. Succinate (500 μM) was incubated with SCR for 2 min prior to EPR measurement at 77 K. (B) Same as A, except that DEANO was included in the mixture at a final concentration of 1 mM. (C) Same as A, except that SCR was pre-incubated with $OONO^-$ (1 mM) for 5 min prior to addition of succinate. (D) Same as C, except that the dosage of $OONO^-$ was increased to 2 mM. EPR parameters: center field, 3401 G; frequency, 9.457 GHz; sweep width, 800 G (only 500 G is shown), power, 20 mM; receiver gain, 1×10^5; modulation amplitude, 5 G; modulation frequency, 100 kHz; conversion time, 150.73 ms/G; time constant, 655.36 ms; number of scans, 5.

of NO may mediate iron depletion from the iron–sulfur cluster through the formation of a dinitrosyl-iron intermediate.

3.8. Effect of $OONO^-$ scavengers on the DEANO induced hydroxyl radical generation by SCR

NO reacts rapidly with $O_2^{\bullet-}$ to produce peroxynitrite ($OONO^-$), which acts as strong oxidant. To test whether $OONO^-$ formation was involved in the molecular mechanism of SCR-mediated hydroxyl radical production induced by DEANO, $OONO^-$ scavengers were employed to inhibit hydroxyl radical generation. As indicated in the Fig. 5B, ebselen (2 μM, a mimic of glutathione peroxidase and can react with $OONO^-$) decreased the detected DEPMPO/$^\bullet$OH by 65%. In the presence of Mn porphyrin (2 μM, MnTMPyP, a cell-permeable superoxide dismutase mimetic which also can scavenges NO), the level of DEPMPO/$^\bullet$OH was inhibited by 76% (Fig. 5C). Uric acid (100 μM, a natural scavenger of $OONO^-$, but not a scavenger for NO) inhibited the level of DEPMPO/$^\bullet$OH by 27% (Fig. 5D). It should be noted that many $OONO^-$ scavengers such as urate may not be highly specific since they also scavenge $NO_2^\bullet$. These data strongly supports the involvement of $OONO^-$ formation in DEANO induced and SCR-mediated hydroxyl radical generation.

3.9. Effect of peroxynitrite ($OONO^-$) on SCR-mediated oxygen-free radical production

It has been reported that addition of $OONO^-$ to isolated mitochondria caused partial inhibition of SQR and SCR [32]. To further explore the role peroxynitrite in the molecular mechanism of SCR-mediated hydroxyl radical production, we incubated SCR (2 μM, based on heme *b*) with $OONO^-$ (50 μM) in PBS. We observed that 25% of the SCR-derived electron transfer activity was irreversibly inhibited by $OONO^-$. When the mixture was activated with succinate in the presence of DEPMPO, a multi-line EPR spectrum was detected (Fig. 6A, solid line). The EPR spectrum was simulated as a combination of two DEPMPO radical adducts (Fig. 6A, dashed line). The first adduct was assigned to DEPMPO/$^\bullet$OOH based on its hyperfine coupling constants: isomer 1 (Fig. 6B): $a^N = 13.14$ G, $a^H_\beta = 11.04$ G, $a^H_\gamma = 0.96$ G, $a^P = 49.96$ G (57.6% relative concentration); isomer 2: $a^N = 13.18$ G, $a^H_\beta = 12.59$ G, $a^H_\gamma = 3.46$ G, $a^P = 48.2$ G (15.4% relative concentration). The second adduct was assigned to DEPMPO/$^\bullet$OH (27% relative concentration; Fig. 6C). Note that catalytic $^\bullet$OH generation mediated by SCR can be detected with a lower $OONO^-$ concentration

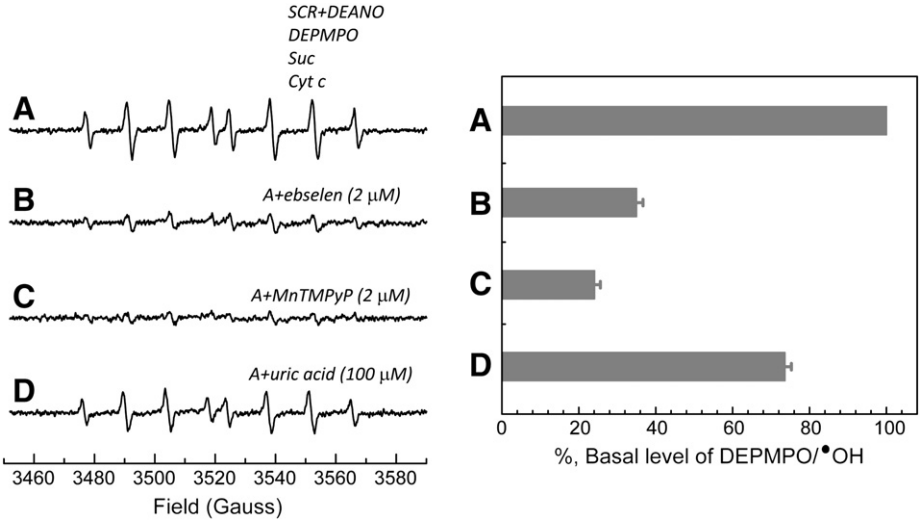

Fig. 5. Effect of $OONO^-$ scavengers on the DEANO induced SCR-mediated hydroxyl radical generation measured by EPR spin trapping with DEPMPO. (A) The reaction mixture contained SCR (2 μM, based on heme *b*) in PBS containing 100 μM DEANO. After pre-incubation at room temperature for 1 min, succinate (18 μM) and cyt *c* (6 μM) were added to initiate the reaction in the presence of DEPMPO (20 mM). EPR spectrum was collected as described in the "Experimental Procedure." (B) Same as A, except that ebselen (2 μM) was included in the reaction mixture. (C) Same as A, except that MnTMPyP (2 μM) was included in the mixture. (D) Same as A, except that uric acid (100 μM) was included in the reaction mixture. Spin quantification was calculated based on the spin number obtained from double integration of simulated spectra.

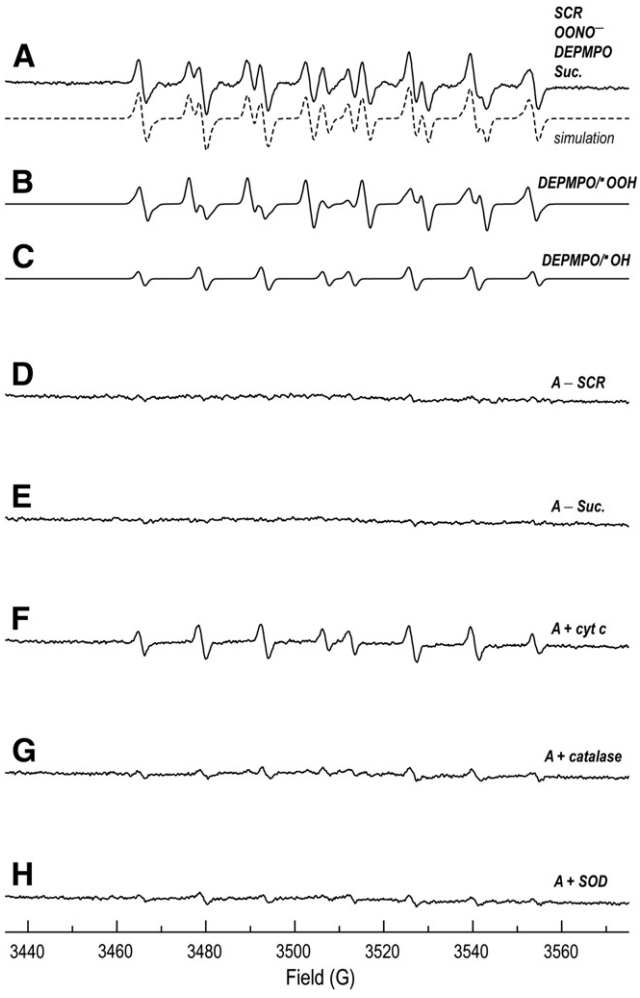

Fig. 6. Radical adducts of DEPMPO/•OH and DEPMPO/•OOH generated from SCR in the presence of peroxynitrite and succinate. (A) The computer simulation (dashed line) superimposed on the experimental spectrum (solid line) obtained using SCR (2 μM), $OONO^-$ (50 μM), succinate (18 μM), and DEPMPO (20 mM) in PBS. $OONO^-$ was premixed with SCR in the presence of spin trap, succinate was immediately added to mixture prior to immediate EPR measurement. The experimental spectrum was recorded after signal averaging 4 scans at room temperature. (B and C) Individual simulations of each species in the composite spectrum. The molar ratio for the two species is 0.73 for DEPMPO/•OOH and 0.27 for DEPMPO/•OH. (D) Same as A, except that SCR was omitted from the system. (E) Same as A, except that succinate was omitted from the system. (F) Same as A, except that cyt *c* (6 μM) was included in the system. (G) Same as A, except that catalase (5 U/μl) was included the system. (H) Same as A, except that SOD (5 U/μl) was included the system.

down to 2.5 μM under the conditions of enzyme turnover in the presence of succinate (20 μM) and cyt *c* (2 μM), thus supporting its pathophysiological relevance (Supplementary Fig. 3).

Catalytic $O_2^{\bullet-}$ generation by SCR decreased gradually with increased $OONO^-$. The relative concentration of DEPMPO/•OH to DEPMPO/•OOH increased proportionally with the amount of $OONO^-$ (data not shown). The production of oxygen-free radical adducts (DEPMPO/•OOH + DEPMPO/•OH) was not detected in the absence of enzyme (Fig. 6D) or in the absence of electron donor (Fig. 6E). In the presence of cyt *c*, $O_2^{\bullet-}$ generation detected as the DEPMPO/•OOH adduct was minimal, and only the DEPMPO/•OH adduct was detected under enzyme turnover conditions (Fig. 6F), indicating that $O_2^{\bullet-}$ produced by SCR was presumably quenched by cyt *c* reduction. Replacement of the cyt *c* in the reaction system with catalase or SOD resulted in a dramatic decrease in the detected oxygen-free radical adducts (Fig. 6G–H), further supporting the involvement of $O_2^{\bullet-}$ and H_2O_2 in the catalytic production of •OH by $OONO^-$-treated SCR.

Effect of $OONO^-$ on the iron sulfur clusters of SCR was further evaluated by low temperature direct EPR at 77 K. The EPR spectrum obtained from $OONO^-$-treated SCR (SCR was mixed with 12.5- and 25-fold excess of $OONO^-$) reduced by succinate indicated diminishing EPR signal intensity of ferredoxin-type iron–sulfur center (decreasing by 35.6% and 79.1% respectively) as shown in the Fig. 4C and D, thus supporting $OONO^-$-mediated destruction of the iron–sulfur cluster of SCR.

3.10. Excess NO increases SCR-mediated oxygen-free radical generation in cardiac myoblast H9c2

Oxaloacetate (OAA) is known as a competitive inhibitor of succinate dehydrogenase (the SDH portion of the SQR) from SCR due to its structural similarity to succinate (see Supplementary Chart). Therefore, in a system of the isolated enzyme complex, SCR-mediated $O_2^{\bullet-}$ production was greatly suppressed by the presence of OAA (Supplementary Fig. 4, upper panel). In the presence of DEANO under the conditions of enzyme turnover, SCR-mediated •OH production was also dramatically inhibited by OAA (Supplementary Fig. 4, lower panel).

To demonstrate whether excess NO can enhance oxygen-free radical production by SCR in living cells, we used confocal microscopy with MitoSOX™ to detect $O_2^{\bullet-}$ in the mitochondria of cardiac myoblasts (H9c2 cell line), and OAA was employed to confirm the state of oxygen-free radical generation catalyzed by SCR in these cells. Note that DAPI staining was used to counter-stain the nuclei (blue). It is well known that antimycin A can induce $O_2^{\bullet-}$ production through enhancement of unstable semiquinone in mitochondria, thus increasing $O_2^{\bullet-}$ production. Therefore, H9c2 cells were treated with antimycin A (10 μM) as a positive control experiment. As indicated in Fig. 7E, a strong red fluorescence from oxidized MitoSOX™ was detected in the antimycin A-treated H9c2 with an enhancement of ~23.0 ± 2.2 fold compared to untreated H9c2. In the control experiment of untreated H9c2, there was almost no detectable red oxidized MitoSOX™ fluorescence (Fig. 7A). However, when the H9c2 cells were treated with DEANO (10 μM) for 20 min, a strong oxidized MitoSOX™ red fluorescence was detected (an enhancement of 22.1 ± 1.8 fold compared to untreated H9c2; Fig. 7B), indicating that excess NO stimulated $O_2^{\bullet-}$ production from the mitochondria of H9c2. Note that 10 μM of DEANO in the Dulbecco's modified Eagle's medium at 37 °C emitted 1.2 μM of NO with a decay rate of 18.8 nM NO/min. Furthermore, treatment of H9c2 with decomposed DEANO (10 μM) or nitrite (10 μM) did not induce detectable oxidized MitoSOX™ red fluorescence (data not shown). The oxidized MitoSOX™ fluorescence induced by DEANO was completely quenched by the NO scavenger c-PTIO (2-(4-carboxyphenyl-4,4,5,5-tetramethylimidazoline-1-oxyl 3-oxide) (Fig. 7C) or the SOD mimetic MnTMPyP (10 μM, data not shown), confirming that it was derived from $O_2^{\bullet-}$ and stimulated by excess NO. Treatment of H9c2 cells with OAA (1 mM), which suppressed the $FADH_2$ formation of SCR, dramatically inhibited the red fluorescence of oxidized MitoSOX™ (~80% inhibition compared to DEANO-treated H9c2; Fig. 7D), thus confirming that excess NO stimulated oxygen-free radicals mediated by the SCR of mitochondrial electron transport chain.

3.11. Excess NO induced SCR-mediated oxygen-free radical generation in endothelial cells (EC) during shear exposure

It is well known that EC exposure to steady laminar shear stress (10 dyn/cm^2, low arterial range) produces NO by activating eNOS via several posttranslational mechanisms and at longer times via eNOS induction [33,34]. In a recent study, Jones et al. reported that mitochondrial $O_2^{\bullet-}$ was produced by ECs sheared at different oxygen tensions (5–21%), the $O_2^{\bullet-}$ production was higher when ECs were sheared at 21%, and the generated $O_2^{\bullet-}$ was linked to the eNOS/NO pathway [35]. We have employed the same cellular system to investigate whether the oxygen-free radical(s) induced by EC shear exposure is mediated by mitochondrial SCR. As indicated in Fig. 8B, shear exposure (at 21% O_2 for 30 min) caused an increase in the

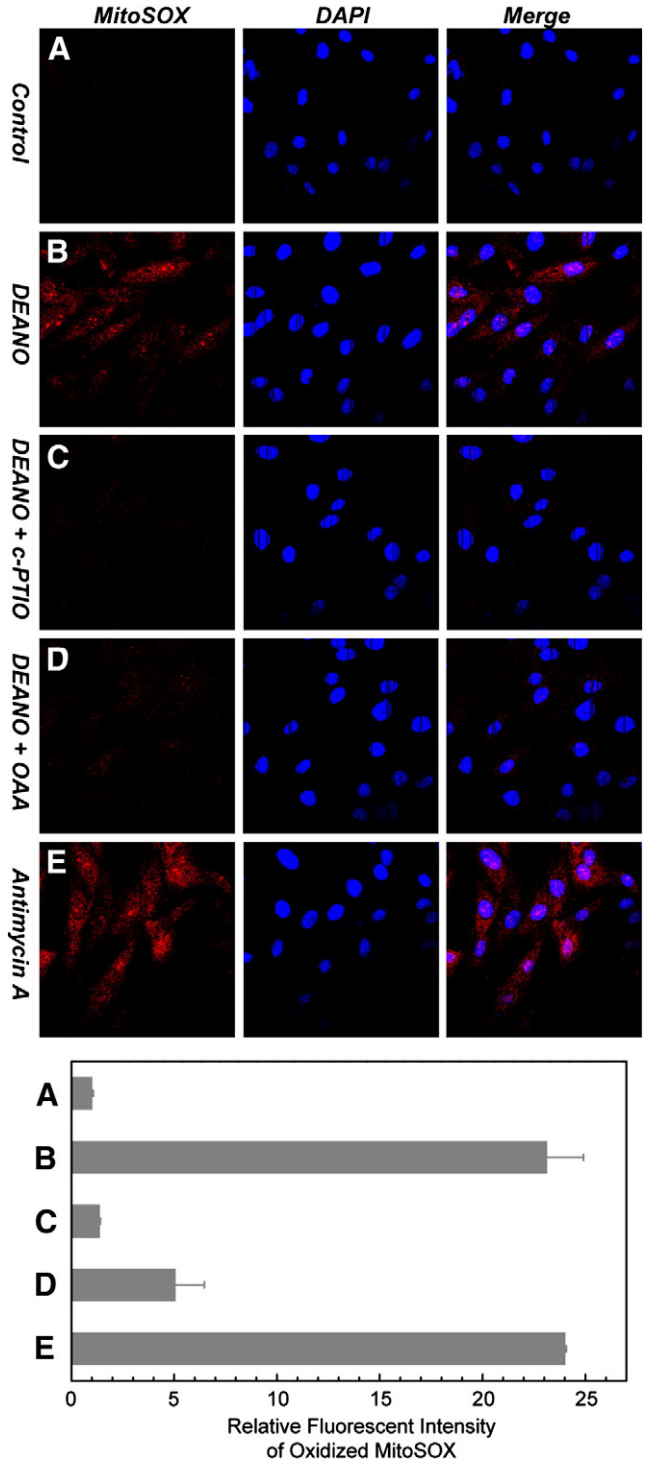

Fig. 7. Imaging of oxygen-free radical generation induced by DEANO in H9c2 cardiac myoblast. (A) Confocal microscopy measurement of oxygen-free radical generation from the culture of H9c2 without treatment. (B) Same as A, except that H9c2 was incubated with DEANO (10 μM). (C) Same as B, except that an NO scavenger, c-PTIO (100 μM), was included in the cell culture. (D) Same as B, except that OAA (1 mM) was included in the cell culture. (E) same as A, except that H9c2 cells were incubated with antimycin A (10 μM). The fluorescent intensity of image was quantitated ($n=3$) with the software of NIS-Elements BR 3.0 (*Nikon Inc.*, Melville, NY).

fluorescence of MitoSOX™ red (an enhancement of ~31.3 ± 0.4 fold compared to static control), as monitored by confocal microscopy, in living ECs. No noticeable increase in MitoSOX™ red fluorescence occurred in a static control maintained at 21% O_2 as shown in Fig. 8A. Pre-incubation and shear at 21% O_2 in the presence of L-NAME (N^G-nitro-L-arginine methyl ester, 1 mM) nearly abolished the MitoSOX™ fluorescence signal (>95% inhibition; Fig. 8C) compared with sheared ECs, implicating that eNOS-mediated NO generation induced by shear exposure contributed to oxygen-free radical production. Pre-incubation and shear at 21% O_2 in the presence of OAA (0.1 mM) significantly decreased the MitoSOX™ fluorescent signal compared with sheared BAECs (>70% inhibition; Fig. 8D), indicating the involvement of SCR in NO-induced mitochondria-derived $O_2^{\bullet-}$ generation occurring during shear exposure.

3.12. Hypoxia/reoxgenation induced SCR-mediated oxygen-free radical generation in cardiac myoblast H9c2

Mitochondria are the major source of oxygen-free radical(s) produced during myocardial ischemia–reperfusion. Myocardial ischemia also provides a stimulus to alter NO metabolism. This alteration upregulates NO production in the myocardium via mediation of NO synthase (NOS)-dependent [11–13,36] and NOS-independent pathways [37,38]. To test whether excess NO produced during ischemia–reperfusion can affect the mitochondria-derived oxygen-free radical production, the H9c2 cell line was subjected to the physiological conditions of hypoxia (H, 1 h) and reoxygenation (RO, 3 min). As indicated in Fig. 9, a strong red fluorescence from oxidized MitoSOX™ was detected in the living H9c2 cells subjected to H/RO. H/RO-induced red fluorescence was quenched in the presence of a SOD mimetic (~70% inhibition; Fig. 9B), confirming that oxygen-free radical(s) were overproduced during I/R. Pre-treatment of H9c2 cells with OAA (1.0 mM) significantly diminished the fluorescent intensity of H/RO-induced oxygen-free radicals (~38% inhibition; Fig. 9C), indicating that mitochondria were involved in the oxygen-free radical production, which was profoundly mediated by SCR. This oxidized MitoSOX™ fluorescence induced by H/RO was partially inhibited by the NOS inhibitor L-NAME (~61% inhibition; Fig. 9D), suggesting that oxygen-free radical production was strongly stimulated by NO generated during H/RO.

4. Discussion

4.1. Mechanism of hydroxyl radical production by SCR in the presence of DEANO

Welter et al. have reported that excess NO moderately inhibited the catalytic function of SCR by blocking the electron transfer activity of SQR [17]. The new finding of this study indicates that interaction of excess NO with SCR predisposed the supercomplex to produce hydroxyl radical, as measured by EPR spin trapping with DEPMPO (Fig. 1A–C). Most hydroxyl radical production by SCR can be inhibited by SOD and catalase, demonstrating that it was linked to the formation of $O_2^{\bullet-}$ intermediate and its derived H_2O_2 (Fig. 1F). As shown by EPR at 77 K, excess NO induced the formation of a dinitrosyl-iron complex at the SQR in the SCR (Fig. 4B). It is likely that formation of a nonheme iron–NO complex in turn blocked electron flow from succinate to cyt *c* and thus stimulated electron leakage from the FAD cofactor for $O_2^{\bullet-}$ generation under the conditions of enzyme turnover (diagram of Fig. 10). $O_2^{\bullet-}$ can be spontaneously dismutated to H_2O_2 ($k=4\times10^5$ M^{-1} s^{-1} at pH 7.4 and Equation 1). However, this reaction (Equation 1) is catalyzed by Mn-SOD at a much faster rate ($k=2\times10^9$ M^{-1} s^{-1} at pH 7.4) in mitochondria.

$$2H^+ + 2O_2^{\bullet-} \rightarrow H_2O_2 + O_2 \quad (1)$$

As shown by EPR spin trapping with DEPMPO, generation of $^{\bullet}OH$ was also inhibited by non-protein (DFO) and protein (apotransferrin) iron chelators (Fig. 1F), indicating the involvement of free Fe^{2+} or Fe^{3+} which was presumably dissociated from the iron–sulfur cluster of SCR. The molecular mechanism of free Fe^{2+} dissociation from the iron sulfur cluster of SQR in the SCR was likely linked to the instability of dinitrosyl

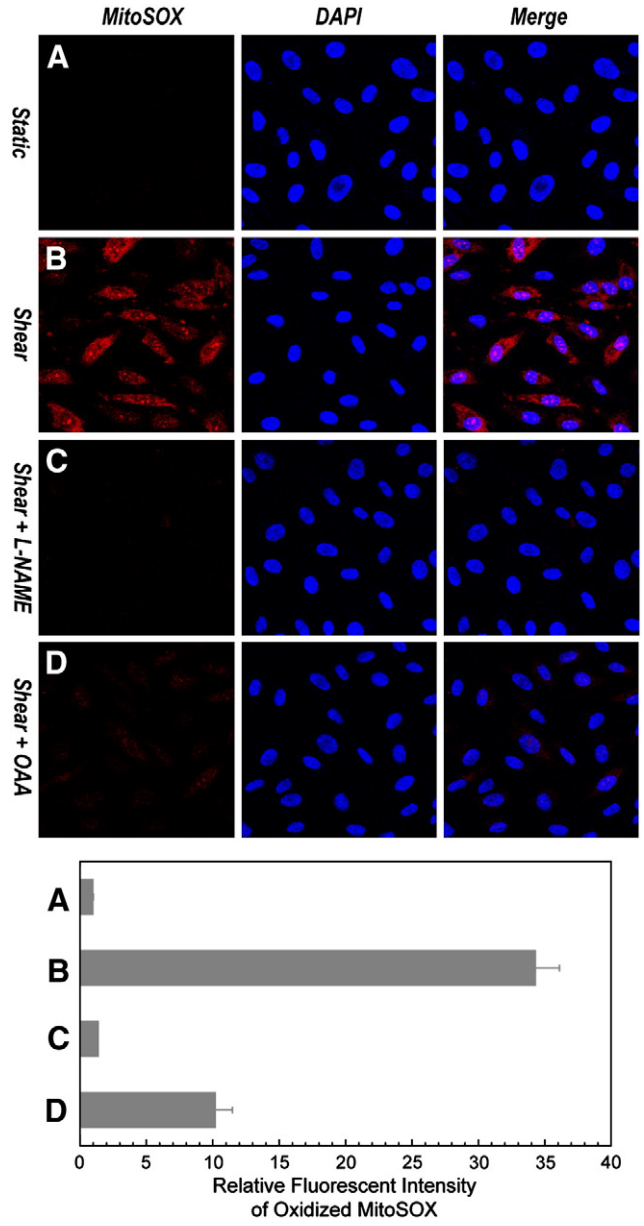

Fig. 8. Oxygen-free radical generation by bovine aortic endothelial cells (BAECs) sheared at 21% O_2. (A) Confocal microscopy measurement of oxygen-free radical generation from the culture of BAECs subjected to static exposure. (B) Same as A, except that BAECs were subjected to shear exposure at 21% O_2. (C) Same as B, except that L-NAME (1 mM) was included in the cell culture. (D) Same as B, except that OAA (0.1 mM) was included in the cell culture. The fluorescent intensity of image was quantitated ($n = 3$) with the software of NIS-Elements BR 3.0 (Nikon Inc., Melville, NY).

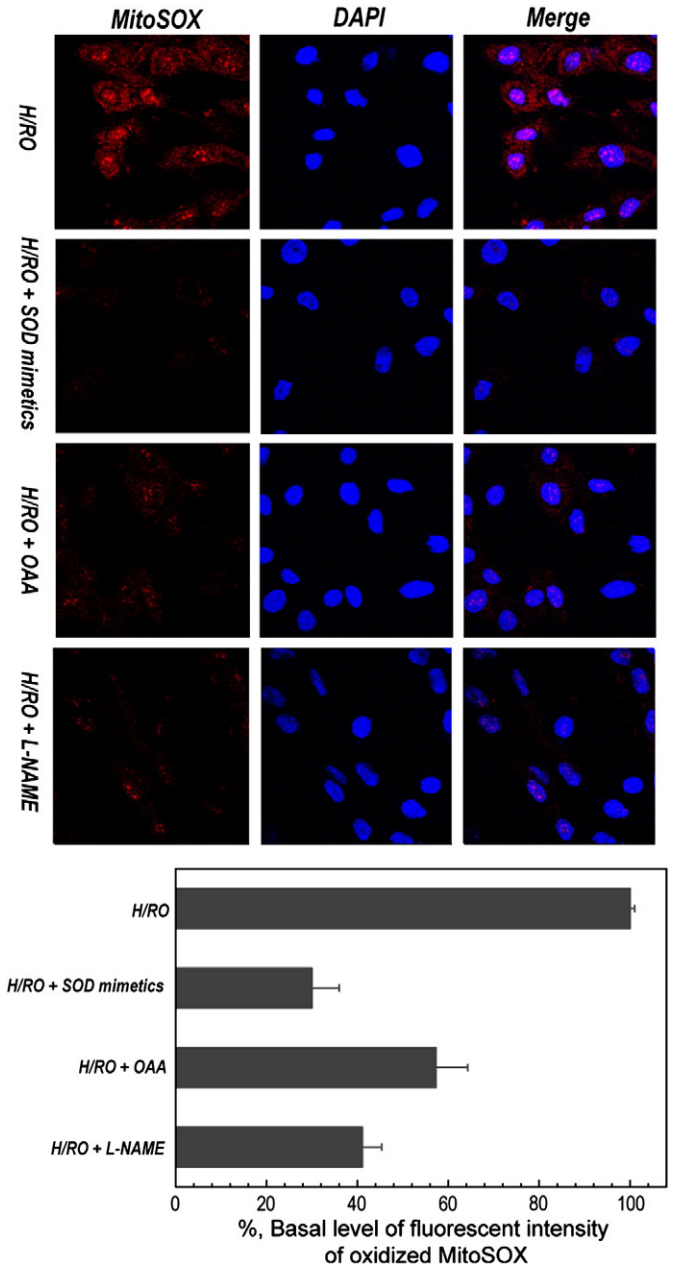

Fig. 9. Imaging of oxygen-free radical generation in H9c2 cardiac myoblast under the conditions of hypoxia/reoxygenation. (A) Confocal microscopy measurement of oxygen-free radical generation from the culture of H9c2 subjected to H/RO. (B) Same as A, except that H9c2 was incubated with the SOD mimetic MnTMPyP (10 μM). (C) Same as A, except that OAA (1 mM) was included in the cell culture. (D) Same as *A*, except that L-NAME (1 mM) was included in the cell culture.

iron intermediate and $O_2^{\bullet-}$-mediated iron sulfur clusters damage. Presumably the excess NO mediates iron depletion from the iron sulfur clusters, leading to impairment of the function of SQR (diagram of Fig. 10). Low levels (20 μM to 1 mM) of succinate generate $O_2^{\bullet-}$ at the FAD cofactor, which then reacts secondary with the free ion released from the damaged iron–sulfur clusters, which would contribute to hydroxyl radical formation. This process changed the iron homeostasis in the enzymatic system and induced $^{\bullet}OH$ generation via the Fe^{2+}-dependent Fenton mechanism (Equation 2) or the Fe^{3+}-catalyzed Haber–Weiss mechanism (Equation 3). Therefore, excess NO predisposed the iron sulfur cluster of SQR in the SCR to be a source of $^{\bullet}OH$.

$$H_2O_2 + Fe^{2+} \rightarrow Fe^{3+} + HO^- + HO^{\bullet} \quad (2)$$

$$H_2O_2 + O_2^{\bullet-} \xrightarrow{Fe^{3+}} O_2 + HO^- + HO^{\bullet} \quad (3)$$

Based on the measurement of EPR spin trapping, ~65% of DEPMPO/$^{\bullet}OH$ adduct from the reaction system was inhibited by SOD (Fig. 1F), suggesting that iron-catalyzed and $O_2^{\bullet-}$-dependent Haber–Weiss mechanism (Equation 3) played a significant role in the SCR-mediated $^{\bullet}OH$ production. Furthermore, SOD-mediated $O_2^{\bullet-}$ dismutation also potentially decreased peroxynitrite formation (even it increases H_2O_2 production), thus restricting the iron depletion from the iron–sulfur cluster and reducing $^{\bullet}OH$ production (vide infra). The residual hydroxyl radical adduct detected was presumably controlled by iron–H_2O_2 Fenton reaction (Equation 2).

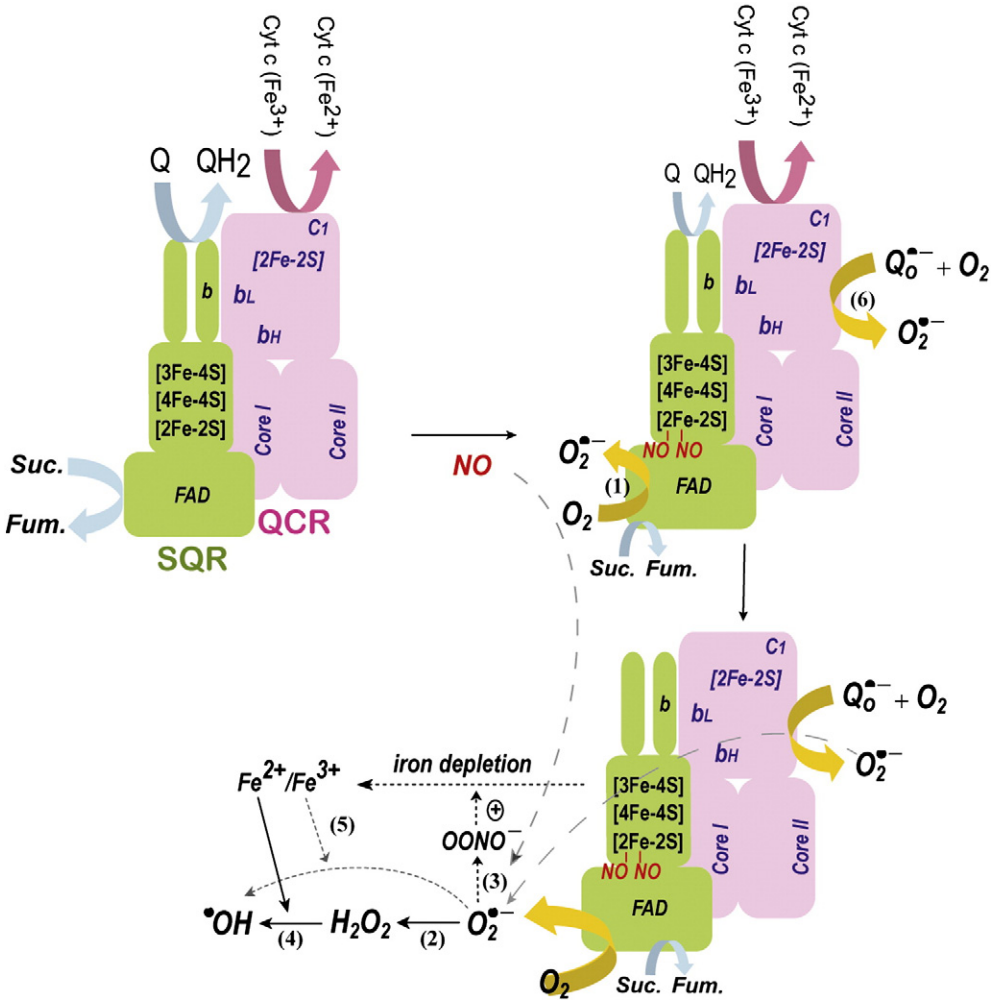

Fig. 10. Diagram showing excess NO production predisposes SCR supercomplex to be a source of hydroxyl radical. Overproduction of NO facilitates the formation of iron–NO complex intermediate at the S1 center [2Fe–2S] of SQR, and subsequently inhibits the electron transfer activity of SQR and stimulates electron leakage from the FAD cofactor for $O_2^{\bullet-}$ production (Reaction 1). $O_2^{\bullet-}$ is spontaneously dismutated to yield H_2O_2 (Reaction 2), or trapped by NO to yield peroxynitrite (Reaction 3) in facilitating iron depletion from iron–sulfur cluster. Hydroxyl radical is thus generated via the Fenton (Reaction 4) or Haber–Weiss mechanism (Reaction 5). $O_2^{\bullet-}$ production is also mediated by the semiquinone at the Q_o site of QCR (Reaction 6).

4.2. Involvement of peroxynitrite

Formation of peroxynitrite was the other mechanism involved since $O_2^{\bullet-}$ can be subsequently trapped by excess NO to generate peroxynitrite at an even higher rate ($k \sim 10^{10}\ M^{-1}\ s^{-1}$). The inhibitory effect of peroxynitrite scavengers (ebselen, MnTMPyP, and uric acid) on the SCR-mediated $^{\bullet}OH$ production supports the above hypothesis (Fig. 5). Peroxynitrite has been reported to mediate iron depletion from the iron sulfur cluster of mitochondrial ETC [14], thus initiating $^{\bullet}OH$ production via Equations 2 and 3. As shown in Fig. 6A, the presence of peroxynitrite in the system (without cyt *c*) induced simultaneous production of $O_2^{\bullet-}$ and $^{\bullet}OH$. The production of $O_2^{\bullet-}$ was derived from the electron leakage of SCR, and $^{\bullet}OH$ should be caused by peroxynitrite-mediated free Fe^{2+}/or Fe^{3+} dissociation from the iron–sulfur cluster of SCR and H_2O_2 derived from spontaneous dismutation of $O_2^{\bullet-}$ (Equation 1). Under the conditions of enzyme turnover, $O_2^{\bullet-}$ was quenched by ferricytochrome *c* (rate constant, $k \sim 10^6\ M^{-1}\ s^{-1}$ [39]) and electron leakage for $O_2^{\bullet-}$ production by SCR was minimized, leading to DEPMPO/$^{\bullet}$OOH as the only product detected in the system (Fig. 6F and Supplementary Fig. 3).

The catalytic efficiency of catalase in H_2O_2 disproportionation (Equation 4) is very high, $k_{cat}/K_M \sim 4.0 \times 10^8 M^{-1}\ s^{-1}$, which is at the diffusion limit. Therefore, the addition of catalase to the reaction system efficiently removed the H_2O_2, leading to diminishing of DEPMPO/$^{\bullet}$OH. Adduct of DEPMPO/$^{\bullet}$OOH was not detected in the presence of catalase (Fig. 6G), presumably because of the slower reaction rate constant ($k \sim 60$–$90\ M^{-1}\ s^{-1}$ [40]) for trapping $O_2^{\bullet-}$ by DEPMPO and because spontaneous dismutation of $O_2^{\bullet-}$ is more efficient than DEPMPO trapping of $O_2^{\bullet-}$.

$$2H_2O_2 \rightarrow 2H_2O + O_2 \quad (4)$$

Failure to detect $O_2^{\bullet-}$ adduct in the reaction system containing Suc/SCR/DEANO/cyt *c*/DEPMPO (Fig. 1A–C) was likely due to trapping of $O_2^{\bullet-}$ by excess NO produced by DEANO, forming the peroxynitrite at a very higher rate (Equation 5, $k \sim 10^{10}\ M^{-1}\ s^{-1}$), which out-competed the slower rate of DEPMPO trapping $O_2^{\bullet-}$. Furthermore, the formation of peroxynitrite may contribute to the iron depletion from the iron sulfur cluster (S3 center of SQR could be the initial center damaged, since it has often been suggested as the most sensitive center to oxidative damage) of SCR, leading to $^{\bullet}OH$ formation through Fenton or Haber–Weiss mechanism.

$$NO + O_2^{\bullet-} \rightarrow OONO^- \quad (5)$$

Protein tyrosine nitration is widely recognized as a fingerprint of peroxynitrite formation. We did not detect the signal of tyrosine nitration of SCR from the reaction system containing SCR, DEANO, succinate, and cyt *c* using a polyclonal antibody against 3-nitrotyrosine in this study (Supplementary Fig. 5, lane 7). Therefore, electron leakage for $O_2^{\bullet-}$ production induced by the formation of iron–NO intermediate

was rapidly trapped by NO, and subsequent peroxynitrite formation should be localized at the iron sulfur clusters of SQR. The effect of peroxynitrite localization would further stimulate iron depletion from the SQR. However, exposure of SCR to peroxynitrite (40–100 μM) under the conditions of enzyme turnover resulted in protein tyrosine nitration at the multiple polypeptides of SCR (Supplementary Fig. 5, lanes, 5, 6, and 8) including the 70 kDa FAD-binding subunit of SQR [32]. Protein nitration of SCR was not detectable when the dosage of peroxynitrite used was below 30 μM (Supplementary Fig. 5, lanes 2–4). Therefore, the peroxynitrite induced by DEANO was not likely sufficient to cause the protein nitration of SCR.

4.3. Involvement of intact supercomplex of SCR

In the system of isolated SQR or isolated QCR, $^{\bullet}OH$ mediated by SQR or QCR in the presence of DEANO was not detected under conditions of enzyme turnover (Fig. 2A and C). Instead, we have observed that excess DEANO suppressed SQR- or QCR-mediated $O_2^{\bullet-}$ generation under the conditions of enzyme turnover (Fig. 2B and D), presumably due to excess NO scavenging of $O_2^{\bullet-}$ produced by SQR or QCR. Reconstitution of SQR and QCR in vitro restored the catalysis of electron transfer from succinate to cyt *c* [16] and thus restored the ability of DEANO to induce hydroxyl radical production under enzyme turnover conditions (Fig. 2G). Therefore, DEANO-stimulated $^{\bullet}OH$ production by SCR is likely in part mediated by QCR due to the requirement of intact supercomplex. Normally $O_2^{\bullet-}$ mediated by SCR is kept minimal under the conditions of enzyme turnover in the presence of succinate and cyt *c* (Figs. 1D and 2F). It should not be ruled out that the formation of the iron–NO complex at the iron sulfur clusters of SQR or oxidative damage of SQR weakens the protein–protein interaction between the SQR and QCR in the supercomplex, and subsequently stimulates QCR-mediated $O_2^{\bullet-}$ production (reaction 6 in Fig. 10), contributing to consequent $^{\bullet}OH$ generation. Note that isolated QCR can generate higher level of $O_2^{\bullet-}$ (measured by EPR spin trapping) than the QCR hosted in the SCR under the conditions in the presence of QH_2 with cyt *c* or without cyt *c* (data not shown).

4.4. Physiological relevance

The impact of excess NO on the mitochondrial respiration of smooth muscle cells has been linked to the impairment of complex II through the mechanism of nitrosylating non-heme iron sulfur proteins [15,19]. Oxidative modification with protein tyrosine nitration occurred at the 70 kDa subunit of complex II was also marked in the post-hypoxic cardiac myocyte [41] and post-ischemic heart [32], and the detected protein tyrosine nitration was presumably caused by overproduction of NO and subsequent peroxynitrite during hypoxia/reoxygeneration. It was also reported that chronic exposure of the endothelium to NO resulted in the destruction of iron homeostasis in mitochondria [42]. In this study, we have demonstrated that excess NO released from DEANO stimulates SCR-mediated oxygen-free radical production in living H9c2 cells and isolated supercomplex (Fig. 7). Similar physiological relevance was further observed in ECs subjected to shear exposure (Fig. 8) and post-hypoxic H9c2 cells (Fig. 9). Therefore, the finding elucidates an important physiological mechanism in controlling oxygen-free radical generation by SCR under the pathological conditions with NO overproduction.

In contrast to normal physiological conditions, production of excess NO has been marked in disease conditions such as myocardial ischemia–reperfusion injury [11]; the markers of NO overproduction, including peroxynitrite-mediated protein nitration, iNOS upregulation, nitrite disproportionation, and eNOS upregulation during blood reflow and subsequent shear exposure, have been demonstrated in systems of myocardial tissue [11,13,36] and ex vivo endothelium [25]. High concentrations of NO and peroxynitrite were expected to block mitochondrial respiration and subsequently stimulate oxygen-free radical production by SCR under the pathological conditions.

4.5. Conclusions

Based on the studies using isolated supercomplex together with physiological alterations detected in the living cells, we delineate a plausible mechanism of correlating SQR-derived iron–NO complex intermediate, peroxynitrite formation, iron depletion, and oxygen-free radical production with the toxicological consequences of excess NO. As illustrated in the diagram of Fig. 10, overproduction of NO facilitates the formation of the iron–NO complex intermediate at the S1 center of SQR, and subsequently enhances electron leakage at the FAD cofactor for $O_2^{\bullet-}$ production (reaction 1 in Fig. 10). $O_2^{\bullet-}$ is spontaneously dismutated to yield H_2O_2 (reaction 2 in Fig. 10), or trapped by NO to yield peroxynitrite (reaction 3 in Fig. 10) in facilitating iron depletion from the iron–sulfur clusters of SQR (Note: S3 center of 3Fe-4 S cluster is most sensitive to ROS). Hydroxyl radical is thus generated via the Fenton (reaction 4 in Fig. 10) or Haber–Weiss mechanisms (reaction 5 in Fig. 10). Therefore, excess NO predisposes SCR to be a hydroxyl radical synthase. This acquired pro-oxidant activity presumably could result from disruption of the iron homeostasis and substrate deprivation in mitochondria under disease conditions. Although the statements that SCR produces hydroxyl radical may be simplification, the finding and elucidation of the above mechanism are important in understanding how NO affects mitochondrial physiology and its related disease pathogenesis. The current in vitro and ex vivo studies thus constitute a valuable model that addresses the molecular mechanism of NO overproduction, implicating it as a cause of oxidative damage under disease conditions. Recognition of this molecular mechanism is important in understanding the fundamental basis by which NO and oxidants modulate cellular injury caused by mitochondrial dysfunction.

Supplementary materials related to this article can be found online at doi:10.1016/j.bbabio.2011.03.001.

Acknowledgements

This work was supported by National Institutes of Health grants HL83237 (to Y-R Chen), HL91417 (to B. R. Alevriadou), HL38324, and HL63744 (to J.L. Zweier). The authors would like to thank Dr. Craig Herman for technical assistance with low temperature EPR and Mr. Randy J. Giedt for technical assistance with the shear experiments.

References

[1] S. Raha, B.H. Robinson, Mitochondria, oxygen free radicals, disease and ageing, Trends Biochem. Sci. 25 (2000) 502–508.
[2] J.F. Turrens, Mitochondrial formation of reactive oxygen species: superoxide production by the mitochondrial respiratory chain, J. Physiol. 552 (2003) 335–344.
[3] J.L. Zweier, J.T. Flaherty, M.L. Weisfeldt, Direct measurement of free radical generation following reperfusion of ischemic myocardium, Proc. Natl Acad. Sci. U.S.A. 84 (1987) 1404–1407.
[4] J.L. Zweier, P. Kuppusamy, R. Williams, B.K. Rayburn, D. Smith, M.L. Weisfeldt, J.T. Flaherty, Measurement and characterization of postischemic free radical generation in the isolated perfused heart, J. Biol. Chem. 264 (1989) 18890–18895.
[5] G. Ambrosio, J.L. Zweier, C. Duilio, P. Kuppusamy, G. Santoro, P.P. Elia, I. Tritto, P. Cirillo, M. Condorelli, M. Chiariello, et al., Evidence that mitochondrial respiration is a source of potentially toxic oxygen free radicals in intact rabbit hearts subjected to ischemia and reflow, J. Biol. Chem. 268 (1993) 18532–18541.
[6] M.J. Curtis, R. Pabla, Nitric oxide supplementation or synthesis block–which is the better approach to treatment of heart disease? Trends Pharmacol. Sci. 18 (1997) 239–244.
[7] S. Lamas, D. Perez-Sala, S. Moncada, Nitric oxide: from discovery to the clinic, Trends Pharmacol. Sci. 19 (1998) 436–438.
[8] M.P. Murphy, Nitric oxide and cell death, Biochim. Biophys. Acta 1411 (1999) 401–414.
[9] P. Liu, C.E. Hock, R. Nagele, P.Y. Wong, Formation of nitric oxide, superoxide, and peroxynitrite in myocardial ischemia-reperfusion injury in rats, Am. J. Physiol. 272 (1997) H2327–H2336.
[10] J.C. Stoclet, B. Muller, K. Gyorgy, R. Andriantsiothaina, A.L. Kleschyov, The inducible nitric oxide synthase in vascular and cardiac tissue, Eur. J. Pharmacol. 375 (1999) 139–155.
[11] P. Wang, J.L. Zweier, Measurement of nitric oxide and peroxynitrite generation in the postischemic heart. Evidence for peroxynitrite-mediated reperfusion injury, J. Biol. Chem. 271 (1996) 29223–29230.

[12] X. Zhao, G. He, Y.R. Chen, R.P. Pandian, P. Kuppusamy, J.L. Zweier, Endothelium-derived nitric oxide regulates postischemic myocardial oxygenation and oxygen consumption by modulation of mitochondrial electron transport, Circulation 111 (2005) 2966–2972.
[13] X. Zhao, Y.R. Chen, G. He, A. Zhang, L.J. Druhan, A.R. Strauch, J.L. Zweier, Endothelial nitric oxide synthase (NOS3) knockout decreases NOS2 induction, limiting hyperoxygenation and conferring protection in the postischemic heart, Am. J. Physiol. Heart Circ. Physiol. 292 (2007) H1541–H1550.
[14] G.C. Brown, Nitric oxide and mitochondrial respiration, Biochim. Biophys. Acta 1411 (1999) 351–369.
[15] Y. Geng, G.K. Hansson, E. Holme, Interferon-gamma and tumor necrosis factor synergize to induce nitric oxide production and inhibit mitochondrial respiration in vascular smooth muscle cells, Circ. Res. 71 (1992) 1268–1276.
[16] Y.R. Chen, C.L. Chen, A. Yeh, X. Liu, J.L. Zweier, Direct and indirect roles of cytochrome b in the mediation of superoxide generation and NO catabolism by mitochondrial succinate–cytochrome c reductase, J. Biol. Chem. 281 (2006) 13159–13168.
[17] R. Welter, L. Yu, C.A. Yu, The effects of nitric oxide on electron transport complexes, Arch. Biochem. Biophys. 331 (1996) 9–14.
[18] N.R. Bastian, C.Y. Yim, J.B. Hibbs Jr., W.E. Samlowski, Induction of iron-derived EPR signals in murine cancers by nitric oxide. Evidence for multiple intracellular targets, J. Biol. Chem. 269 (1994) 5127–5131.
[19] Y.J. Geng, A.S. Petersson, A. Wennmalm, G.K. Hansson, Cytokine-induced expression of nitric oxide synthase results in nitrosylation of heme and nonheme iron proteins in vascular smooth muscle cells, Exp. Cell Res. 214 (1994) 418–428.
[20] L. Yu, C.A. Yu, Quantitative resolution of succinate–cytochrome c reductase into succinate-ubiquinone and ubiquinol-cytochrome c reductases, J. Biol. Chem. 257 (1982) 2016–2021.
[21] Y.R. Chen, C.L. Chen, X. Liu, H. Li, J.L. Zweier, R.P. Mason, Involvement of protein radical, protein aggregation, and effects on NO metabolism in the hypochlorite-mediated oxidation of mitochondrial cytochrome c, Free Radic. Biol. Med. 37 (2004) 1591–1603.
[22] D.R. Duling, Simulation of multiple isotropic spin-trap EPR spectra, J. Magn. Reson. B 104 (1994) 105–110.
[23] Y.R. Chen, C.L. Chen, L. Zhang, K.B. Green-Church, J.L. Zweier, Superoxide generation from mitochondrial NADH dehydrogenase induces self-inactivation with specific protein radical formation, J. Biol. Chem. 280 (2005) 37339–37348.
[24] C. Frejaville, H. Karoui, B. Tuccio, F. Le Moigne, M. Culcasi, S. Pietri, R. Lauricella, P. Tordo, 5-(Diethoxyphosphoryl)-5-methyl-1-pyrroline N-oxide: a new efficient phosphorylated nitrone for the in vitro and in vivo spin trapping of oxygen-centered radicals, J. Med. Chem. 38 (1995) 258–265.
[25] Z. Han, Y.R. Chen, C.I. Jones III, G. Meenakshisundaram, J.L. Zweier, B.R. Alevriadou, Shear-induced reactive nitrogen species inhibit mitochondrial respiratory complex activities in cultured vascular endothelial cells, Am. J. Physiol. Cell Physiol. 292 (2007) C1103–C1112.
[26] B.J. Reeder, M.T. Wilson, Desferrioxamine inhibits production of cytotoxic heme to protein cross-linked myoglobin: a mechanism to protect against oxidative stress without iron chelation, Chem. Res. Toxicol. 18 (2005) 1004–1011.
[27] M.A. Sharpe, C.E. Cooper, Reactions of nitric oxide with mitochondrial cytochrome c: a novel mechanism for the formation of nitroxyl anion and peroxynitrite, Biochem. J. 332 (1998) 9–19.
[28] F. Sun, X. Huo, Y. Zhai, A. Wang, J. Xu, D. Su, M. Bartlam, Z. Rao, Crystal structure of mitochondrial respiratory membrane protein complex II, Cell 121 (2005) 1043–1057.
[29] K.R. Messner, J.A. Imlay, Mechanism of superoxide and hydrogen peroxide formation by fumarate reductase, succinate dehydrogenase, and aspartate oxidase, J. Biol. Chem. 277 (2002) 42563–42571.
[30] T. Ohnishi, J.C. Salerno, Thermodynamic and EPR characteristics of two ferredoxin-type iron–sulfur centers in the succinate-ubiquinone reductase segment of the respiratory chain, J. Biol. Chem. 251 (1976) 2094–2104.
[31] J.C. Salerno, T. Ohnishi, Tetranuclear and binuclear iron–sulfur clusters in succinate dehydrogenase: a method of iron quantitation by formation of paramagnetic complexes, Biochem. Biophys. Res. Commun. 73 (1976) 833–840.
[32] C.L. Chen, J. Chen, S. Rawale, S. Varadharaj, P.P. Kaumaya, J.L. Zweier, Y.R. Chen, Protein tyrosine nitration of flavin subunit is associated with oxidative modification of mitochondrial complex II in the post-ischemic myocardium, J. Biol. Chem. 283 (2008) 27991–28003.
[33] Z.G. Jin, H. Ueba, T. Tanimoto, A.O. Lungu, M.D. Frame, B.C. Berk, Ligand-independent activation of vascular endothelial growth factor receptor 2 by fluid shear stress regulates activation of endothelial nitric oxide synthase, Circ. Res. 93 (2003) 354–363.
[34] M.J. Kuchan, J.A. Frangos, Role of calcium and calmodulin in flow-induced nitric oxide production in endothelial cells, Am. J. Physiol. 266 (1994) C628–C636.
[35] C.I. Jones III, Z. Han, T. Presley, S. Varadharaj, J.L. Zweier, G. Ilangovan, B.R. Alevriadou, Endothelial cell respiration is affected by the oxygen tension during shear exposure: role of mitochondrial peroxynitrite, Am. J. Physiol. Cell Physiol. 295 (2008) C180–C191.
[36] J.L. Zweier, P. Wang, A. Samouilov, P. Kuppusamy, Enzyme-independent formation of nitric oxide in biological tissues, Nat. Med. 1 (1995) 804–809.
[37] J.L. Zweier, A. Samouilov, P. Kuppusamy, Non-enzymatic nitric oxide synthesis in biological systems, Biochim. Biophys. Acta 1411 (1999) 250–262.
[38] J.L. Zweier, P. Wang, P. Kuppusamy, Direct measurement of nitric oxide generation in the ischemic heart using electron paramagnetic resonance spectroscopy, J. Biol. Chem. 270 (1995) 304–307.
[39] J. Butler, W.H. Koppenol, E. Margoliash, Kinetics and mechanism of the reduction of ferricytochrome c by the superoxide anion, J. Biol. Chem. 257 (1982) 10747–10750.
[40] F.A. Villamena, J.L. Zweier, Detection of reactive oxygen and nitrogen species by EPR spin trapping, Antioxid. Redox Signal. 6 (2004) 619–629.
[41] L. Zhang, C.L. Chen, P.T. Kang, V. Garg, K. Hu, K.B. Green-Church, Y.R. Chen, Peroxynitrite-mediated oxidative modifications of complex II: relevance in myocardial infarction, Biochemistry 49 (2010) 2529–2539.
[42] A. Ramachandran, E. Ceaser, V.M. Darley-Usmar, Chronic exposure to nitric oxide alters the free iron pool in endothelial cells: role of mitochondrial respiratory complexes and heat shock proteins, Proc. Natl Acad. Sci. USA 101 (2004) 384–389.